Journal of Photochemistry and Photobiology A: Chemistry 208 (2009) 21–26

Contents lists available at ScienceDirect

Journal of Photochemistry and Photobiology A: Chemistry

journal homepage: www.elsevier.com/locate/jphotochem

Intramolecular energy transfer in 3-amino-*N*-(7′-methoxy-4′-methylcoumaryl)phthalimide

Manabu Nakazono[a], Kenichiro Saita[b,c], Chika Kurihara[a], Shinkoh Nanbu[b,1], Kiyoshi Zaitsu[a,*]

[a] Graduate School of Pharmaceutical Sciences, Kyushu University, 3-1-1 Maidashi, Higashi-ku, Fukuoka 812-8582, Japan
[b] Research Institute for Information Technology, Kyushu University, 6-10-1 Hakozaki, Higashi-ku, Fukuoka 812-8581, Japan
[c] Graduate School of Science, Kyushu University, 6-10-1 Hakozaki, Higashi-ku, Fukuoka 812-8581, Japan

ARTICLE INFO

Article history:
Received 14 April 2009
Received in revised form 13 July 2009
Accepted 29 July 2009
Available online 5 August 2009

Keywords:
Fluorescence
Intramolecular energy transfer
Coumarin
Phthalimide

ABSTRACT

The synthesis and fluorescence property of 3-amino-*N*-(7′-methoxy-4′-methylcoumaryl)phthalimide (AMMP) are described. The fluorescence of AMMP originated during the intramolecular energy transfer from the coumarin moiety to the phthalimde moiety in various solvents. The ab initio quantum chemical calculation of the AMMP revealed that the HOMO and LUMO of AMMP were localized in the coumarin and phthalimide moieties, respectively.

1. Introduction

Various coumarin derivatives are practically used as ion-responsive fluorescence (FL) compounds [1,2] and FL labeling reagents of carboxylic acids [3–6]. However, the FL maximum wavelength and intensity of most coumarin derivatives are short and low. When these disadvantages of the FL properties of the coumarin derivatives are alleviated, the utilities of the coumarin derivatives as FL reagents will increase. Recently, FL probes have been synthesized on the basis of the FL energy transfer (ET) [7–10], photoinduced electron transfer (PeT) [11] and charge transfer (CT) [12]. Thus, we focused on the intramolecular ET to have a longer FL maximum wavelength and to increase the FL intensity. To achieve this, the two following conditions were required. The first one is that the emission spectrum of the coumarin moiety and the excitation spectrum of the phthalimide moiety should overlap. The FL excitation and emission maximum (Ex(max), Em(max)) wavelengths of 7-methoxy-4-methylcoumarin (7M4MC) and 3-aminophthalimide (3AP) in CH_3OH were as follows: 7M4MC: Ex(max) 320 nm, Em(max) 381 nm; 3AP: Ex(max) 385 nm, Em(max) 475 nm. The second one is that the acceptor having a stronger FL and a higher FL quantum yield than those of the coumarin moiety should be selected. The FL intensity of 3AP was stronger than that of 7M4MC in CH_3OH (Fig. 1). The FL quantum yield (Φ_F) of 3AP was 0.54 in CH_3OH. 7M4MC and 3AP are compounds which meet two conditions described above. Thus, the conjugate of 7M4MC and 3AP should exhibit an intramolecular ET from the coumarin moiety to the phthalimide moiety. We newly synthesized the 3-amino-*N*-(7′-methoxy-4′-methylcoumaryl)phthalimide (AMMP, Scheme 1), and measured the FL and FL lifetime. An ab initio calculation was also performed to evaluate the theoretical treatment of the FL property of AMMP.

2. Experimental

2.1. Materials

Deionized and distilled water purified by a Milli-QII (Japan Millipore, Tokyo, Japan) was used. 4-Bromomethyl-7-methoxycoumarin was purchased from Tokyo Kasei Kogyo (Tokyo, Japan). 7-Methoxy-4-methylcoumarin was purchased from Wako Pure Chemical Industries, Ltd (Osaka, Japan). 3-Aminophthalimide was purchased from Kodak (New York, USA). All other chemicals and solvents were of analytical reagent grade.

2.2. Apparatus

Column chromatography was performed using silica gel 60N (63–210 μm, Kanto Chemical Co., Inc., Tokyo, Japan). The ^{1}H NMR

Abbreviations: FL, fluorescence; ET, energy transfer; Ex(max), excitation maximum; Em(max), emission maximum.

* Corresponding author. Tel.: +81 92 642 6596; fax: +81 92 642 6601.
E-mail address: zaitsu@phar.kyushu-u.ac.jp (K. Zaitsu).
[1] Present address: Department of Materials and Life Sciences, Faculty of Science and Technology, Sophia University, 7-1 Kioi-cho, Chiyoda-ku, Tokyo 102-8554, Japan.

1010-6030/$ – see front matter © 2009 Elsevier B.V. All rights reserved.
doi:10.1016/j.jphotochem.2009.07.028

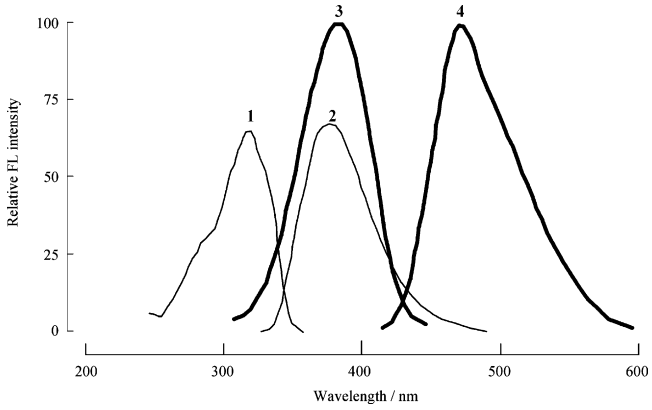

Fig. 1. The FL excitation and emission spectra of 7M4MC and 3AP. Curves 1 and 2 show the FL excitation and emission spectra of 7M4MC. Curves 3 and 4 show the FL excitation and emission spectra of 3AP. The concentration of 7M4MC and 3AP in CH_3OH is 1 μM.

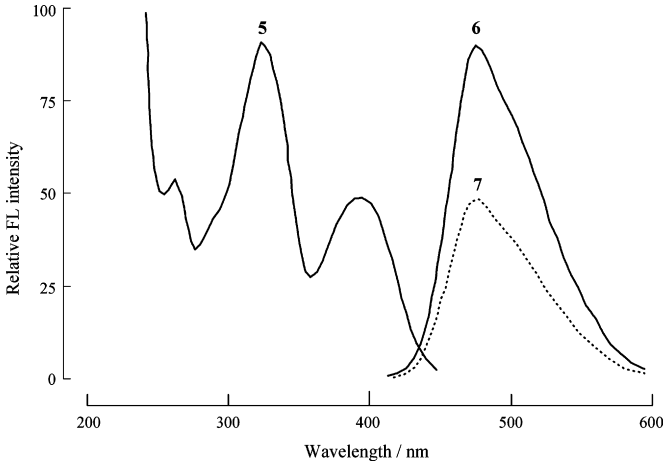

Fig. 2. The FL excitation and emission spectra of AMMP in CH_3OH. Curve 5 shows the FL excitation spectrum of AMMP. Curves 6 and 7 show the FL emission spectra of AMMP at the excitation wavelength of 322 nm or 391 nm, respectively. The concentration of AMMP was 1 μM in CH_3OH.

spectrum of AMMP was recorded by a Varian UNITY plus (USA) spectrometer at 500 MHz. The FAB MS of AMMP was obtained using a JEOL JMS 600 (Tokyo, Japan). The absorption and fluorescence spectra of 7M4MC, 3AP and AMMP were obtained using a Jasco V-530 absorptiometer and FP-6500 fluorometer (Tokyo, Japan). All the FL spectra were corrected. A fluoroCube (3000U, HoribaJobin-YvonIBH, Kyoto, Japan) was used to measure the FL lifetime by the time-correlated single photon counting (TCSPC) method. NanoLED340 or 370 was used as light source.

2.3. Synthesis of AMMP (Scheme 1)

To stirred dimethylformamide (30 ml) were added 3-aminophthalimide (0.16 g, 1 mmol), K_2CO_3 (1.5 g) and 4-bromomethyl-7-methoxycoumarin (0.27 g, 1 mmol). The mixture was refluxed for 2 h, filtered and H_2O (150 mL) was then added. The organic layer was extracted with ethyl acetate (300 mL). The solution was dried with anhydrous Na_2SO_4. The filtrate was concentrated and purified by column chromatography ($CHCl_3$:CH_3OH = 20:1 → $CHCl_3$ → $CHCl_3$:Hexane = 10:1) to give AMMP as a yellow powder (0.05 g, 14.3% yield, mp 266 °C). ^1H NMR ($(CD_3)_2S$=O): 3.87 (s, 3H, OCH_3), 4.9 (s, 2H, –N–CH_2–), 6 (s, 1H, ArH), 6.5 (brs, 1H, ArH), 7 (m, 3H, ArH), 7.45 (t, 1H, J = 7.5 Hz, ArH), 7.86 (d, 1H, J = 8.5 Hz, ArH). FAB MS: 351.10 $[M+H]^+$, Anal. Calcd. for $C_{19}H_{14}N_2O_5$: C, 65.14; H, 4.03; N, 8.00. Found: C, 65.27; H, 4.04; N, 7.82.

2.4. Computational methods

The equilibrium geometry of the electronic ground (S_0) state of AMMP was fully optimized by the CASPT2 ab initio MO calculations [13]. In each step of the optimization, the potential energies and the natural orbitals were obtained from the three-state-averaged multi-configuration self-consistent field (MCSCF) with the complete active space (CASSCF) calculations [14], and then the potential energies were revised by subsequent multireference perturbation calculations using the second-order Rayleigh–Schrödinger perturbation theory (RS2). These CASPT2 calculations were performed using the electronic structure program MOLPRO (revision 2006.1) [15]. Dunning's cc-pVDZ (correlation consistent, polarized valence, double zeta) basis set was used [16] in all the calculations described above.

3. Results and discussion

3.1. The FL wavelength and intensity of 7M4MC, 3AP and AMMP

Compared to the FL excitation and emission spectra of 7M4MC and 3AP, the FL emission spectrum of 7M4MC overlapped with the FL excitation spectrum of 3AP (Fig. 1). As shown in Fig. 2, the FL Ex(max) and Em(max) wavelengths of AMMP were 322 nm and 480 nm, respectively. When AMMP was excited at 391 nm, the FL Em(max) wavelength was 479 nm. Thus the intramolecular ET from the coumarin moiety to the phthalimide moiety occurred. The FL spectra of 7M4MC (Ex(max) 320 nm), 3AP (Ex(max) 381 nm) and AMMP (Ex(max) 322 nm) in CH_3OH are shown in Fig. 3. The FL intensity (Ex(max) 322 nm, Em(max) 480 nm) of AMMP was 3.9-fold higher than that of 7M4MC (Ex(max) 320 nm, Em(max) 381 nm). The FL intensity (Ex(max) 322 nm, Em(max) 480 nm) of AMMP was 39-fold higher than that of 3AP (Ex(max) 320 nm, Em(max) 476 nm) (Table 1). Thus the FL intensity of 3AP (Ex(max) 320 nm) was very low and did not affect the FL intensity of AMMP (Ex(max) 322 nm). These similar FL properties of AMMP were

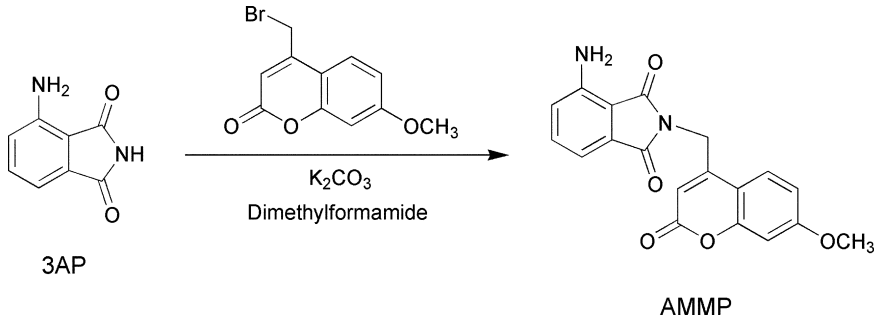

Scheme 1. Synthesis of 3-amino-*N*-(7′-methoxy-4′-methylcoumaryl)phthalimide (AMMP).

Table 1
The FL properties of 7M4MC, 3AP and AMMP in (a) CH_3OH or (b) CH_3CN.

Compound[a]	ε (M^{-1} cm^{-1})	Ex(max) (nm)	Em(max) (nm)	Apparent Stokes' shift (nm)	ϕ_F[b]	Relative fluorescence intensity[c]	
(a) CH_3OH							
7M4MC	15,120	320	381	61	0.1	1	
3AP	370	320	476	156		0.1	1
	4210	385	476	91	0.54	1.5	
AMMP	14,390	322	480	158	0.53	3.9	39
	6050	391	479	88		2.1	
(b) CH_3CN							
7M4MC	13,550	318	379	61	0.02	1	
3AP	440	318	452	134		0.9	1
	4220	378	453	75	0.65	14.6	
AMMP	12,750	320	464	144	0.64	37.1	41
	5540	385	465	80		21	

[a] The concentration of 7M4MC, 3AP and AMMP was 1 μM.
[b] Quantum yield (Quinine sulfate in 0.05 M H_2SO_4, $\Phi = 0.51$).
[c] The FL intensity of 7M4MC or 3AP (Ex. 320 nm in CH_3OH or Ex. 318 nm in CH_3CN) was taken as 1.

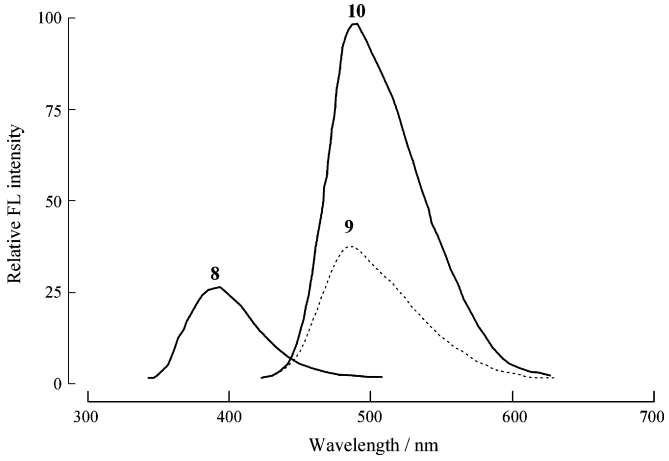

Fig. 3. The FL emission spectra of 7M4MC, 3AP and AMMP in CH_3OH. Curves 8, 9 and 10 show the FL emission spectra of 7M4MC, 3AP and AMMP. The excitation wavelengths of 7M4MC, 3AP and AMMP were 320 nm, 385 nm or 322 nm. The concentration of 7M4MC, 3AP and AMMP was 1 μM in CH_3OH.

observed in CH_3CN (Table 2), ethanol, ethyl acetate, dimethylformamide, dimethylsulfoxide, and 50% (v/v) dimethylsulfoxide–H_2O. The FL intensity of AMMP in CH_3CN was the strongest among tested all the solvents. In AMMP, the FL Em(max) wavelength shifted to a longer value and the FL intensity was stronger than that of 7M4MC.

3.2. The FL lifetimes and quantum yields of 7M4MC, 3AP and AMMP, and the intramolecular ET efficiency of AMMP

The FL lifetime and quantum yield of 7M4MC, 3AP and AMMP were measured to show the intramolecular ET of AMMP. The FL lifetimes of 7M4MC, 3AP and AMMP in CH_3OH were 0.42 ns, 13.9 ns and 13.6 ns, respectively (Table 2(a)). The FL lifetime of AMMP (Ex. 333 nm) in CH_3OH was much longer than that of 7M4MC (Table 2(a)). The FL lifetime of AMMP was similar to that of 3AP when AMMP or 3AP was excited at 333 nm in CH_3OH or CH_3CN. The FL lifetimes of AMMP (Ex. 373 nm) in CH_3OH or CH_3CN were 13.8 ns and 13.1 ns, respectively, and were similar to that of 3AP (Table 2). The FL quantum yield (Φ_F) of 3AP and AMMP in CH_3OH was 0.54 and 0.53, respectively (Table 1(a)). The FL quantum yield (Φ_F) of 3AP and AMMP in CH_3CN was 0.65 and 0.64, respectively (Table 1(b)). Therefore, the intramolecular ET from the coumarin moiety to the phthalimide moiety occurs in AMMP. The intramolecular ET efficiency of AMMP in CH_3OH was calculated using the following equations [8,9]:

J: overlap integral (M^{-1} cm^3), F_D: donor FL per unit wavelength interval, ε_A: molar absorptivity of acceptor (M^{-1} cm^{-1}), λ: wavelength (cm).

$$J = \int F_D(\lambda)\varepsilon_A(\lambda)\lambda^4 d\lambda \quad (1)$$

R_0: Förster distance (Å), κ^2: Förster orientation factor (2/3), n: refractive index of solvent (1.33), Q_D: quantum yield of donor.

$$R_0 = 9.78 \times 10^2 (k^2 n^{-4} Q_D J)^{1/6} \quad (2)$$

k_T: rate of energy transfer (ns^{-1}), τ_D: FL lifetime of the donor in the absence of the acceptor (ns), r: distance between donor and acceptor (Å), E: ET efficiency.

$$k_T = \frac{1}{\tau_D} \times \left(\frac{R_0}{r}\right)^6 \quad (3)$$

$$E = \frac{k_T}{(\tau_D^{-1} + k_T)} \quad (4)$$

Table 2
The FL lifetime of 7M4MC, 3AP and AMMP in (a) CH_3OH or (b) CH_3CN. The concentration of 7M4MC, 3AP and AMMP was 10 μM.

	Ex(max) (nm)	Em(max) (nm)	FL lifetime (ns)
(a) CH_3OH			
7M4MC	333	381	0.42
3AP	373	476	13.9
AMMP	333	480	13.6
	373	476	13.8
(b) CH_3CN			
7M4MC	333	379	Not detected
3AP	373	453	12.9
AMMP	333	464	13.3
	373	453	13.1

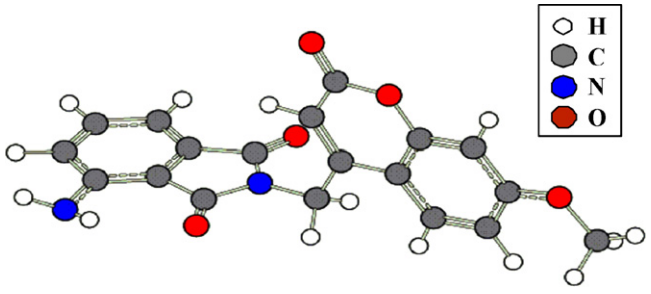

Fig. 4. The optimized structure of AMMP.

Table 3
The potential energies and the electron configurations of the low-lying electronic excited states of AMMP obtained by the CASPT2/cc-pVDZ calculations. The oscillator strength in the row of S_1 and S_2 corresponds to the S_1–S_0 and the S_2–S_0 photoexcitation, respectively.

	Electronic state	E (cm^{-1})	Electron configuration (coefficients of CI expansion)		Oscillator strength
AMMP	S_0	0	$(88a)^2(89a)^2(90a)^2(91a)^2(92a)^0(93a)^0$	(0.9749230)	
	S_1	36,188	$(88a)^2(89a)^2(90a)^1(91a)^2(92a)^1(93a)^0$	(0.9318600)	0.30408
			$(88a)^2(89a)^1(90a)^1(91a)^2(92a)^2(93a)^0$	(0.1920526)	
	S_2	46,238	$(88a)^2(89a)^2(90a)^2(91a)^1(92a)^0(93a)^1$	(0.9518215)	0.65379
			$(88a)^1(89a)^2(90a)^2(91a)^1(92a)^0(93a)^2$	(0.1808339)	

$J = 6.36 \times 10^{-15}$ (M^{-1} cm^3), $R_0 = 22.2$ (Å), $k_T = 2.42 \times 10^{12}$ (s^{-1}), $E = 99\%$. The intramolecular ET efficiency of AMMP was very high. The Em(max) wavelengths of AMMP excited at Ex(max) wavelengths of 7M4MC and 3AP were almost the same. The Φ_F of AMMP and 3AP, and the FL lifetimes of AMMP and 3AP were almost the same (Tables 1 and 2). Furthermore, the spectral overlap of the FL emission spectrum of 7M4MC and the excitation spectrum of 3AP was observed (Fig. 1). We proposed that these factors related with the high intramolecular ET efficiency of AMMP.

3.3. Computational analysis

The optimized structure of AMMP is shown in Fig. 4. This right-angled-twisted structure corresponds to the equilibrium geometry of the S_0 state. The center-to-center distance of the coumarin moiety and phthalimide moiety is 6–7 Å, and this short distance is needed to produce the high intramolecular ET efficiency of AMMP. Table 3 displays the potential energies of the lowest electronic excited (S_1) and the second-lowest (S_2) states, and the electron configurations which mostly contribute to those states. For the S_1 state, the single electron excitation, $(90a)^1 \rightarrow (92a)^1$, is the primary configuration and the double excitation, $(89a)^1(90a)^1 \rightarrow (92a)^2$, is secondary. For the S_2 state, on the other hand, the primary and secondary configurations are $(91a)^1 \rightarrow (93a)^1$ and $(88a)^1(91a)^1 \rightarrow (93a)^2$, respectively. The relationship of the oscillator strengths of the S_0–S_1 and S_0–S_2 excitations well reproduce the ratio of the absorption intensities shown in Table 1 or Fig. 2, and figure out that the S_0–S_2 transition is dominant when AMMP is excited at 322 nm irradiation. The low-energy natural orbitals of AMMP obtained from the MCSCF calculation are depicted in Fig. 5. Since the optimized geometry has about 90 degree dihedral angle of the coumarin and the phthalimide ring, LUMO + 1 (*93a*), HOMO (*91a*) and HOMO-3 (*88a*) are localized completely on the coumarin moiety in the analogous fashion to the LUMO, the HOMO, and the HOMO-1 of isolated 7M4MC, respectively. Simultaneously, LUMO (*92a*), HOMO-1 (*90a*) and HOMO-2 (*89a*) are similar to the LUMO, the HOMO, and HOMO-1 of 3AP molecule, respectively. Because of the MO structure, the electronic transitions between the MOs localized on the different parts would be optically forbidden; the oscillator strength of the S_2–S_1 transition is 0.0011. However, the twisting motions of the molecule in solution could produce the overlap of the orbitals as shown in Fig. 6. In addition, the energy gap between the S_1 and S_2 decreases down to ~230 cm^{-1} on the condition of 45 degree torsion. These features of the electronic structure of AMMP suggest that the intramolecular

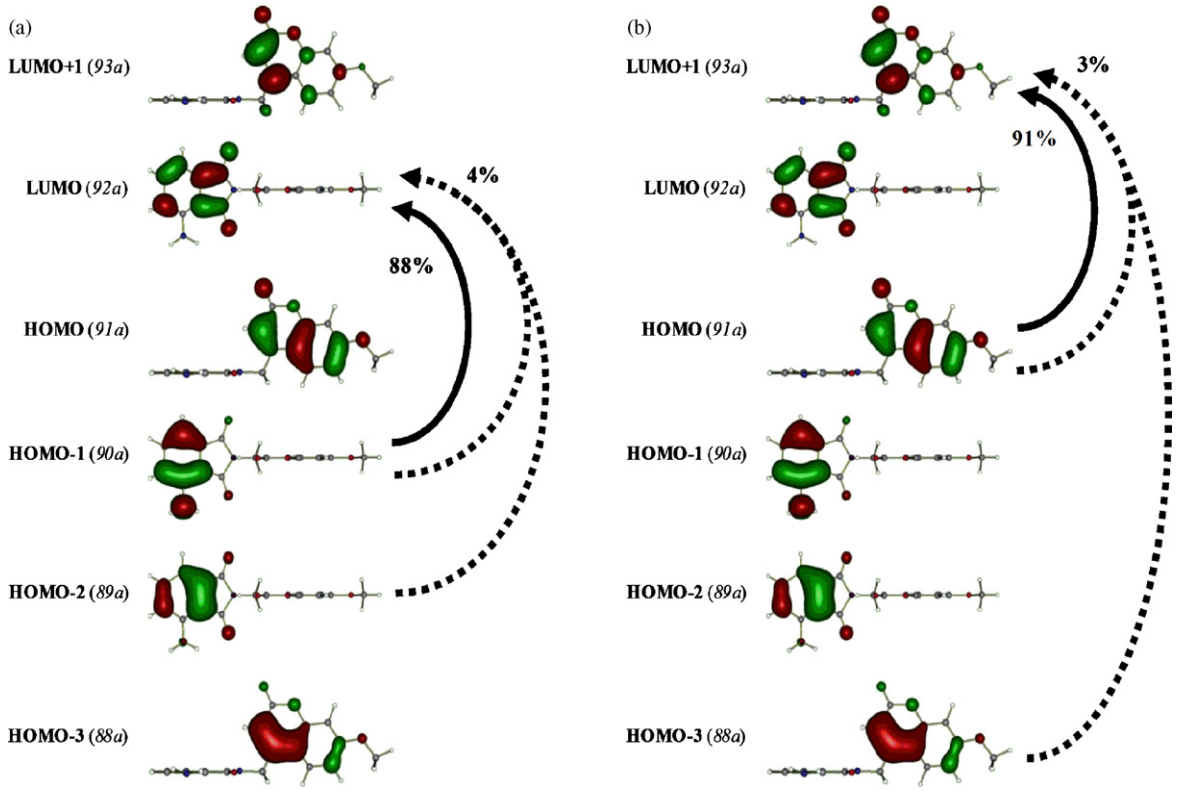

Fig. 5. Low-energy MOs of AMMP obtained from MCSCF calculation and schematic representation of the electron configurations of (a) the S_1 state and (b) the S_2 state. Arrow with solid line and with two broken lines intends primary and secondary configurations respectively. Figures with percent (%) intend their contribution for the states. See also Table 3.

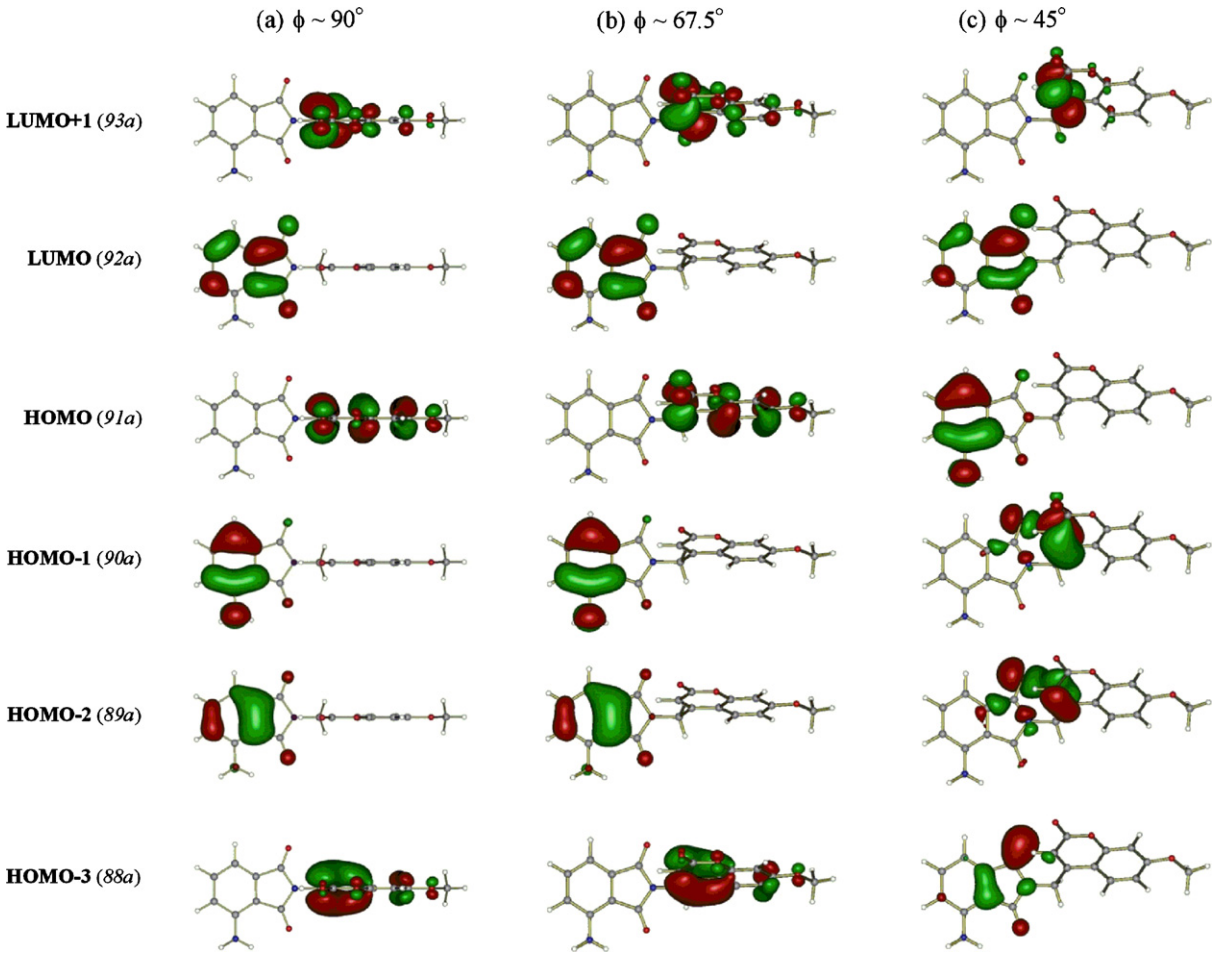

Fig. 6. Change of the low-lying MOs of AMMP with the torsion of the coumarin and phthalimide moieties.

ET from the coumarin moiety to the phthalimide moiety particularly occurs following the S_2–S_0 excitation.

4. Conclusions

A new fluorescent conjugate, 3-amino-*N*-(7′-methoxy-4′-methylcoumaryl)phthalimide (AMMP) was synthesized. And it was clarified that AMMP fluoresced by transferring energy efficiently from the coumarin moiety to the phthalimide moiety in various solvents. The ab initio quantum chemical calculation of AMMP suggested the intramolecular ET of AMMP. 7M4MC and 3AP are excellent donor and acceptor, respectively. This result provides a practical method to have a longer FL maximum wavelength and to increase the FL intensity.

Acknowledgments

We thank Prof. Dr. Fuyuki Ito, Graduate School of Engineering, Kyushu University, and Prof. Dr. Takeharu Nagai, Research Institute for Electronic Science, Hokkaido University for their helpful discussion on intramolecular ET. The computation was mainly performed at the computer facilities at the Research Center for Computational Science of The Okazaki National Institutes. We thank Horiba, Ltd. (Kyoto, Japan), for the FL lifetime measurements.

References

[1] J. Bourson, M.-N. Borrel, J.B. Valeur, Ion-responsive fluorescent compounds. Part 3. Cation complexation with coumarin 153 linked to monoaza-15-crown-5, Anal. Chim. Acta 257 (1992) 189–193.
[2] J. Bourson, J. Pouget, B. Valeur, Ion-responsive fluorescent compounds. 4. Effect of cation binding on the photophysical properties of a coumarin linked to monoaza- and diaza-crown ethers, J. Phys. Chem. 97 (1993) 4552–4557.
[3] W. Dünges, 4-Bromomethyl-7-methoxycoumarin as a new fluorescence label for fatty acids, Anal. Chem. 49 (1977) 442–445.
[4] E. Grushka, S. Lam, J. Chassin, Fluorescence labeling of dicarboxylic acids for high performance liquid chromatographic separation, Anal. Chem. 50 (1978) 1398–1399.
[5] A. Takadate, T. Masuda, C. Tajima, C. Murata, M. Irikura, S. Goya, 4-Bromoacetyl-7-methoxycoumarin as a new fluorescent derivatization reagent for carboxylic acids in high-performance liquid chromatography, Anal. Sci. 8 (1992) 663–668.
[6] A. Takadate, T. Masuda, C. Murata, C. Haratake, A. Isobe, M. Irikura, S. Goya, 4-Bromoacetyl-6,7-methylenedioxycoumarin as a highly reactive and sensitive fluorescence labeling reagent for fatty acids, Anal. Sci. 8 (1992) 695–697.
[7] G.S. Jiao, A. Loudet, H.B. Lee, S. Kalinin, L.B.-Å. Johansson, K. Burgess, Synthesis and spectroscopic properties of energy transfer systems based on squaraines, Tetrahedron 59 (2003) 3109–3116.
[8] J.N. Miller, Fluorescence energy transfer methods in bioanalysis, Analyst 130 (2005) 265–270.
[9] D.L. Andrews, A.A. Demidov, Resonance Energy Transfer, John Wiley & Sons Ltd, 1999.
[10] N. Kuznetsova, D. Makarov, V. Derkacheva, L. Savvina, V. Alekseeva, L. Marinina, L. Slivka, O. Kaliya, E. Lukyanets, Intramolecular energy transfer in rhodamine–phthalocyanine conjugates, J. Photochem. Photobiol. A: Chem. 200 (2008) 161–168.
[11] E. Sasaki, H. Kojima, H. Nishimatsu, Y. Urano, K. Kikuchi, Y. Hirata, T. Nagano, Highly sensitive near-infrared fluorescent probes for nitric oxide and their application to isolated organs, J. Am. Chem. Soc. 127 (2005) 3684–3685.
[12] A. Wakamiya, K. Mori, S. Yamaguchi, 3-Boryl-2,2′-bithiophene as a versatile core skeleton for full-color highly emissive organic solids, Angew. Chem. Int. Ed. 46 (2007) 4273–4276.
[13] H.-J. Werner, Third-order multireference perturbation theory. The CASPT3 method, Mol. Phys. 89 (1996) 645–661.
[14] (a) H.-J. Werner, P.J. Knowles, A second order multiconfiguration SCF procedure with optimum convergence, J. Chem. Phys. 82 (1985) 5053–5063;

(b) P.J. Knowles, H.-J. Werner, An efficient second-order MCSCF method for long configuration expansions, Chem. Phys. Lett. 115 (1985) 259–267.
[15] H.-J. Werner, P.J. Knowles, R. Lindh, F.R. Manby, M. Schütz, P. Celani, T. Korona, G. Rauhut, R.D. Amos, A. Bernhardsson, A. Berning, D.L. Cooper, M.J.O. Deegan, A.J. Dobbyn, F. Eckert, C. Hampel, G. Hetzer, A.W. Lloyd, S.J. McNicholas, W. Meyer, M.E. Mura, A. Nicklass, P. Palmieri, R. Pitzer, U. Schumann, H. Stoll, A.J. Stone, R. Tarroni, T. Thorsteinsson, MOLPRO, version 2006.1, a package of ab initio programs (http://www.molpro.net).
[16] D.E. Woon, T.H. Dunning Jr., Gaussian basis sets for use in correlated molecular calculations. III. The atoms aluminum through argon, J. Chem. Phys. 98 (1993) 1358–1371.